



**CHALMERS**  
UNIVERSITY OF TECHNOLOGY

## **Hampered PdO Redox Dynamics by Water Suppresses Lean Methane Oxidation over Realistic Palladium Catalysts**

Downloaded from: <https://research.chalmers.se>, 2026-04-10 16:23 UTC

Citation for the original published paper (version of record):

Velin, P., Hemmingsson, F., Schaefer, A. et al (2021). Hampered PdO Redox Dynamics by Water Suppresses Lean Methane Oxidation over Realistic Palladium Catalysts. *ChemCatChem*, 13(17): 3765-3771. <http://dx.doi.org/10.1002/cctc.202100829>

N.B. When citing this work, cite the original published paper.

# Hampered PdO Redox Dynamics by Water Suppresses Lean Methane Oxidation over Realistic Palladium Catalysts

Peter Velin,<sup>[a]</sup> Felix Hemmingsson,<sup>[a]</sup> Andreas Schaefer,<sup>[a]</sup> Magnus Skoglundh,<sup>[a]</sup> Kirill A. Lomachenko,<sup>[b]</sup> Agnes Raj,<sup>[c]</sup> David Thompsett,<sup>[c]</sup> Gudmund Smedler,<sup>[d]</sup> and Per-Anders Carlsson<sup>\*[a]</sup>

By use of *operando* spectroscopies under cycling reaction conditions, water is shown to hamper the redox dynamics of realistic palladium oxide nanoparticles dispersed onto alumina and hydrophobic zeolite supports thereby lowering the activity for total oxidation of methane. Water adsorption forms hydroxyl ad-species that block the methane and oxygen dissociation and seem to prevent lattice oxygen to take part in the methane oxidation. The main catalytic action is thus proposed to shift from the Mars-van Krevelen mechanism in dry conditions to a slower route that relies on Langmuir-Hinshelwood type of steps in wet conditions. This key finding has clear implications on catalyst design for low-temperature gas combustion emission control.

Methane (CH<sub>4</sub>) is the second most important greenhouse gas contributor to climate change and a potent local air pollutant giving rise to formation of ground-level ozone.<sup>[1,2]</sup> In view of this, the efficiency of heterogeneous catalyst technologies for total oxidation of methane has in recent years been deemed necessary to improve as to be useful for end-of-pipe methane emission control applications.<sup>[3,4]</sup> Even when using the most active supported palladium-based catalysts known hitherto,<sup>[5–7]</sup> the desired practical methane conversion is often difficult to achieve because water inhibits the methane oxidation, effectively, at all temperatures from which methane starts to be

converted to as high as 550 °C.<sup>[8–15]</sup> The problem is obvious for gas combustion exhaust aftertreatment as water concentrations may reach well over 10% by volume.<sup>[16]</sup> Over the last decades, the development of methane oxidation catalysts has faced a weak progress as compared to, e.g., catalysts for abatement of nitrogen oxides emissions.<sup>[17]</sup> Among the strategies for improving methane conversion one finds, on the one hand, various catalyst designs including alloying palladium with platinum<sup>[18,19,20]</sup> and use of reducible supports<sup>[18,21,22]</sup> and, on the other hand, utilization of gas composition changes.<sup>[18,23,24]</sup> Despite these efforts, it is clear that new fundamental understanding is necessary to advance the technology.<sup>[25]</sup> To this end, we have used *in situ* diffuse reflectance infrared Fourier transform spectroscopy (DRIFTS) and synchrotron-based *operando* energy-dispersive X-ray absorption spectroscopy (ED-XAS) under pulsed oxygen (O<sub>2</sub>) and water (H<sub>2</sub>O) flow conditions to address the impact of water on the ability of supported PdO particles to interact with CH<sub>4</sub> and O<sub>2</sub> as well as catalyse the CH<sub>4</sub> oxidation reaction. We show that water hampers the catalyst redox dynamics leading to decreased catalytic activity for CH<sub>4</sub> oxidation likely through alternating the operating mechanism.

To achieve practical relevance, realistic palladium-based catalysts were prepared by industrially recognized methods. Four different catalysts with 1.7–1.8 wt.% Pd dispersed onto alumina (γ-Al<sub>2</sub>O<sub>3</sub>) and highly siliceous MFI zeolite (ZSM-5, SiO<sub>2</sub>/Al<sub>2</sub>O<sub>3</sub> = 2000) supports were prepared by incipient wetness impregnation using nitrate and non-nitrate palladium precursor solutions as to deliberately achieve for both supports high and low Pd dispersion, respectively. Apart from the resulting physicochemical properties described hereunder, the precursors are not expected to lead to other differences of significance for catalyst efficiency. The physicochemical properties of the catalysts were characterized by X-ray fluorescence (XRF), nitrogen sorption (BET), carbon monoxide (CO) chemisorption, X-ray diffraction (XRD), transmission electron microscopy (TEM) and *in situ* DRIFTS with CO adsorption as detailed in Supporting Information and summarized in Table 1. The catalysts are denoted PdAl<sub>D57%</sub>, PdAl<sub>D14%</sub>, PdZ<sub>D21%</sub> and PdZ<sub>D5.2%</sub> where Al stands for alumina, Z for ZSM-5 and subscripts the obtained Pd dispersion. The Pd dispersion, mean Pd particle size and total Pd surface area were all determined from the CO uptake together with individual stoichiometric factors (F<sub>S</sub>) for CO adsorption assuming hemispherical particles and a Pd site area of 7.87 Å.<sup>[2,26]</sup> The F<sub>S</sub> describes how CO binds to the surface palladium atoms and considers the relative proportions of linear, bridge and threefold hollow bonded CO<sup>[27–29]</sup> obtained

[a] Dr. P. Velin, F. Hemmingsson, Dr. A. Schaefer, Prof. M. Skoglundh, Prof. P.-A. Carlsson

Department of Chemistry and Chemical Engineering  
Chalmers University of Technology  
412 96 Gothenburg (Sweden)

E-mail: per-anders.carlsson@chalmers.se

[b] Dr. K. A. Lomachenko

European Synchrotron Radiation Facility  
38043 Grenoble Cedex 9 (France)

[c] Dr. A. Raj, Dr. D. Thompsett

Johnson Matthey Technology Centre  
Blounts Court

RG4 9NH Sonning Common, Reading (UK)

[d] Dr. G. Smedler

Johnson Matthey AB  
421 31 Västra Frölunda (Sweden)

Supporting information for this article is available on the WWW under <https://doi.org/10.1002/cctc.202100829>

© 2021 The Authors. ChemCatChem published by Wiley-VCH GmbH. This is an open access article under the terms of the Creative Commons Attribution Non-Commercial NoDerivs License, which permits use and distribution in any medium, provided the original work is properly cited, the use is non-commercial and no modifications or adaptations are made.

**Table 1.** Summary of catalyst characteristics including Pd loading, specific surface area (SSA), CO uptake by chemisorption at 35 °C, stoichiometric factor ( $F_5$ ), i.e., surface Pd:CO ratio at CO saturation at 35 °C, palladium dispersion ( $D_{Pd}$ ), palladium surface area ( $A_{Pd}$ ), palladium particle size ( $d_{Pd}$ ), palladium oxide particle size ( $d_{PdO}$ ).

Sample ID	Pd load <sup>[a]</sup> [wt.%]	SSA [m <sup>2</sup> g <sup>-1</sup> ]	CO uptake [μmol g <sup>-1</sup> ]	$F_5$ <sup>[b]</sup>	$D_{Pd}$ [%]	Pd area [m <sup>2</sup> g <sup>-1</sup> ]	$d_{Pd}$ [nm]	$d_{PdO}$ [nm]
PdAl <sub>D57%</sub>	1.7 ± 0.1	142 ± 0.3	43 ± 0.5	2.1	57	4.3	2.0	–
PdAl <sub>D14%</sub>	1.8 ± 0.1	131 ± 0.4	11 ± 0.2	2.2	14	1.1	8.0	18
PdZ <sub>D21%</sub>	1.8 ± 0.1	387 ± 0.7	18 ± 0.3	2.0	21	1.7	5.4	–
PdZ <sub>D5.2%</sub>	1.7 ± 0.1	368 ± 0.7	4.1 ± 0.3	2.0	5.2	0.39	22	37

[a] Determined by XRF. [b] Obtained from deconvoluted IR spectra (see Figure 1)

from Voigt fitting and deconvolution of CO absorption infrared vibrational spectra<sup>[14,30]</sup> (Figure 1e–h) assuming negligible differences in the carbonyl extinction coefficients.<sup>[31]</sup> The CO uptake numbers correspond well to the carbonyl spectra. The PdAl<sub>D57%</sub> catalyst takes up most CO and shows a pre-eminent build-up of carbonyls. The mean Pd particle size is 2.0, 8.0, 5.4 and 22 nm for the PdAl<sub>D57%</sub>, PdAl<sub>D14%</sub>, PdZ<sub>D21%</sub> and PdZ<sub>D5.2%</sub> catalysts, respectively. The average particle sizes are supported by the TEM images (Figure 1a–d) showing as prepared PdO particles and their particle-size distribution (inserts), which is rather broad for the low-dispersed samples. Further, using the Sherrer equation at full width at half maximum (FWHM) values of the PdO(101) reflection at  $2\theta = 34^\circ$  in the XRD patterns (Figure 1i), reveals PdO particle sizes slightly larger than the average sizes for the PdAl<sub>D14%</sub> and PdZ<sub>D5.2%</sub> samples, which is reasonable given the necessary condition of long-range order for clear diffraction. For the same reason, the highly dispersed samples give no clear diffraction.

We start off the discussion on water inhibition by comparing the general catalytic behaviour of the catalysts and tie this to previous literature. The two well-dispersed catalysts show higher catalytic activity in terms of methane conversion during dry conditions (*cf.*  $t = 0\text{--}0.5$  h in Figure 2a) primarily thanks to the presence of a larger number of active sites as compared to the low-dispersed counterparts. The water sensitivity of supported palladium catalysts depends on palladium particle size<sup>[15]</sup> but is also much dependent on the choice of support material.<sup>[16,32,33]</sup> As can be seen, when 10% H<sub>2</sub>O is introduced ( $t = 0.5$  h) to the lean CH<sub>4</sub>/O<sub>2</sub> mixture, the methane conversion drops for both  $\gamma$ -Al<sub>2</sub>O<sub>3</sub> and the hydrophobic ZSM-5 supported palladium, present as PdO particles under prevailing conditions.<sup>[34–36]</sup> The drop is considerably more severe for the alumina catalysts, signifying a higher sensitivity towards water in line with previous works.<sup>[6]</sup> When water is removed from the feed ( $t = 24.5$  h), the conversion is rapidly restored nearly in full for the ZSM-5 catalysts whereas for the alumina catalysts it is only partially recovered. These observations suggest that for zeolite catalysts, the conversion is determined primarily by competitive adsorption of the main reactants and water on the active sites such that when dry condition is reintroduced, the catalytic activity is quickly restored as opposed to the alumina catalysts for which the initial activity can be re-established only by high-temperature treatment in dry conditions (not shown). We mention that for palladium-alumina systems, the Pd particle size should not exceed about 2 nm as to balance palladium

utilization and water inhibition.<sup>[15]</sup> The different response to water is further visualized by the DRIFTS spectra for lean CH<sub>4</sub> oxidation in dry-wet-dry conditions shown in Figure 2 for the alumina (panel b and d) and zeolite (panel c and e) catalysts. On the alumina catalyst, spill-over of hydrogen-containing species form hydroxyl ad-species with various configurations presumably close to the PdO particles already at the start with dry conditions. When water is introduced, a considerable build-up of surface hydroxyls occurs also on the extended alumina surface (spectators) giving rise to highly intense IR bands due to various hydroxyl species. The bands at 3770, 3732, 3694, 3555 and 3501 cm<sup>-1</sup> correspond to terminal OH to octacoordinated Al on (100) surface,<sup>[37,38]</sup> bridged OH to pentacoordinated Al on (111) surface,<sup>[37,38]</sup> bridged OH to octacoordinated Al on (110) surface,<sup>[38–40]</sup> triple-bridged OH to octacoordinated Al on (100) surface<sup>[37,38]</sup> and perturbed terminal OH,<sup>[41,42]</sup> respectively. We mention that hydroxyls on PdO cannot be resolved with certainty in this measurement, however, highly active sites, likely present at the rim of the PdO particles, are clearly inhibited.<sup>[14,15,43]</sup> The hydroxyls on the extended alumina surface may function as a reservoir that supply hydroxyl ad-species to otherwise active sites impeding the reaction for sustained times after water is removed from the feed. A deeper discussion of rim sites and routes for hydroxyl formation is presented in previous systematic studies.<sup>[14,15]</sup> The zeolite catalyst responds in stark contrast to the alumina catalyst in that hydroxyl formation could hardly be detected neither in dry nor wet conditions. This is an important explanation for the higher water tolerance and rapid recovery from wet conditions of zeolite supported PdO catalysts. Still, the zeolite systems are affected by presence of water and, hence, water impacts on crucial surface processes also on those PdO particles.

To shine light on how water impacts the ability of alumina and zeolite supported PdO particles to interact with CH<sub>4</sub> and O<sub>2</sub>, and catalyse the CH<sub>4</sub> oxidation, we have qualitatively correlated Pd chemical state to methane turn-over frequency (CH<sub>4</sub>-TOF) by use of *operando* ED-XAS according to established practice at beamline ID24 at the European Synchrotron Radiation Facility, Grenoble, France.<sup>[44]</sup> The CH<sub>4</sub>-TOF is calculated based on the number of palladium sites determined from the individual CO uptake numbers and  $F_5$  in line with previous works.<sup>[14]</sup> The higher CH<sub>4</sub>-TOFs for the zeolite catalysts compared to alumina catalysts is owing to the use of CH<sub>4</sub>-TOF reflecting site activity. From a system perspective, using CH<sub>4</sub> conversion (per Pd loading) as a measure on catalytic activity, the highly dispersed

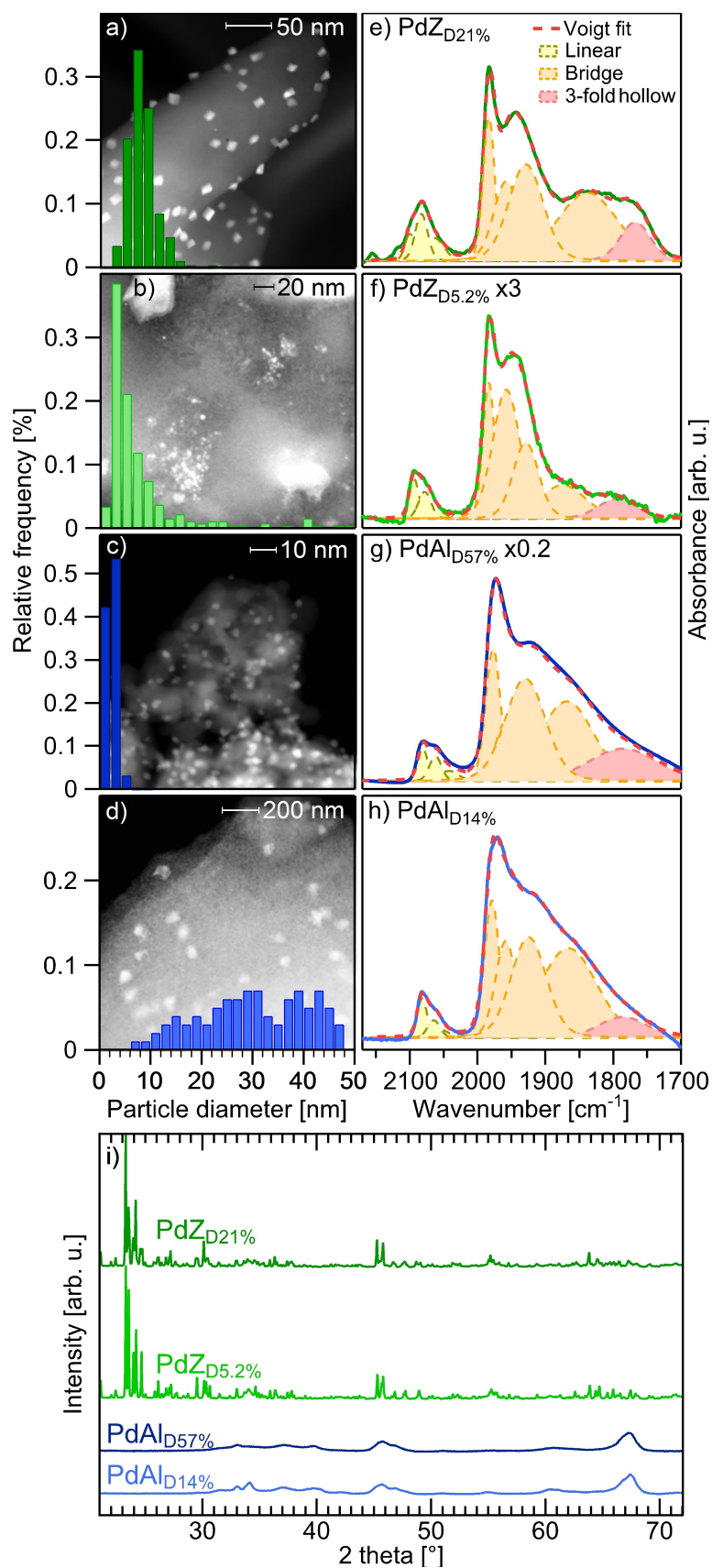


**Figure 1.** Transmission electron microscopy images with palladium particle size distribution as inserts and *in situ* CO infrared absorption spectra deconvoluted into linear, bridge and three-fold hollow CO binding configurations for the PdZn<sub>D21%</sub> (a and e) PdZn<sub>D5.2%</sub> (b and f), PdAl<sub>D57%</sub> (c and g) and PdAl<sub>D14%</sub> (d and h) samples, and X-ray diffraction patterns for all samples (i).

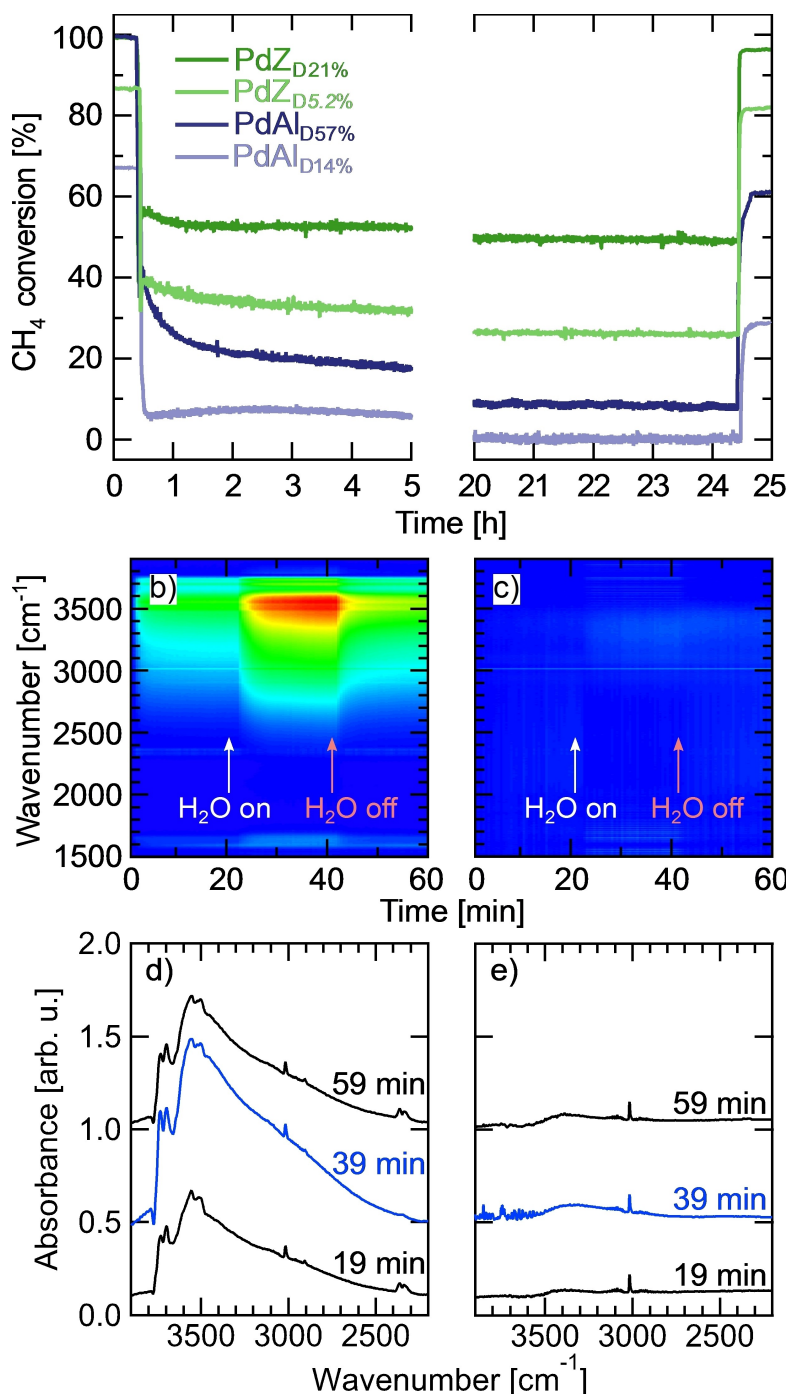


**Figure 2.** Methane conversion as a function of time during oxidation of 0.1% CH<sub>4</sub> with 2% O<sub>2</sub> over the PdZ<sub>D21%</sub>, PdZ<sub>D5.2%</sub>, PdAl<sub>D57%</sub> and PdAl<sub>D14%</sub> at 400 °C in the absence (0–0.5 and 24.5–25 h) and presence (0.5–24.5 h) of 10% H<sub>2</sub>O in the feed (panel a) and color maps (red = high intensity, blue = low intensity) and selected spectra of *in situ* DRIFTS measurements for PdAl<sub>D57%</sub> (panel a and d) and PdZ<sub>D21%</sub> (panel c and e) catalysts during oxidation of 0.1% CH<sub>4</sub> with 2% O<sub>2</sub> adding/removing 2% H<sub>2</sub>O from the feed at 300 °C.

alumina catalyst would appear most efficient in dry conditions as seen in Figure 2a. However, we stress that the following discussion and conclusions are not dependent on choice of measure of catalytic activity. Rather we show that for all these catalysts, water addition is of major importance and the behaviour of each catalyst can be judged on its own through the systematic use of the following gas composition sequences.

Imposing perturbed reaction conditions, i.e., O<sub>2</sub> pulses to a CH<sub>4</sub>/He mixture (reference measurement), O<sub>2</sub> pulses to a CH<sub>4</sub>/H<sub>2</sub>O/He mixture and H<sub>2</sub>O pulses to a lean CH<sub>4</sub>/O<sub>2</sub>/He mixture using a portable water generator,<sup>[45]</sup> the redox dynamics of the particles could be followed *in operando*. In Figure 3, the variations in CH<sub>4</sub>-TOF and Pd K-edge white-line intensity (WLI) are shown for all catalysts under the mentioned perturbed conditions at

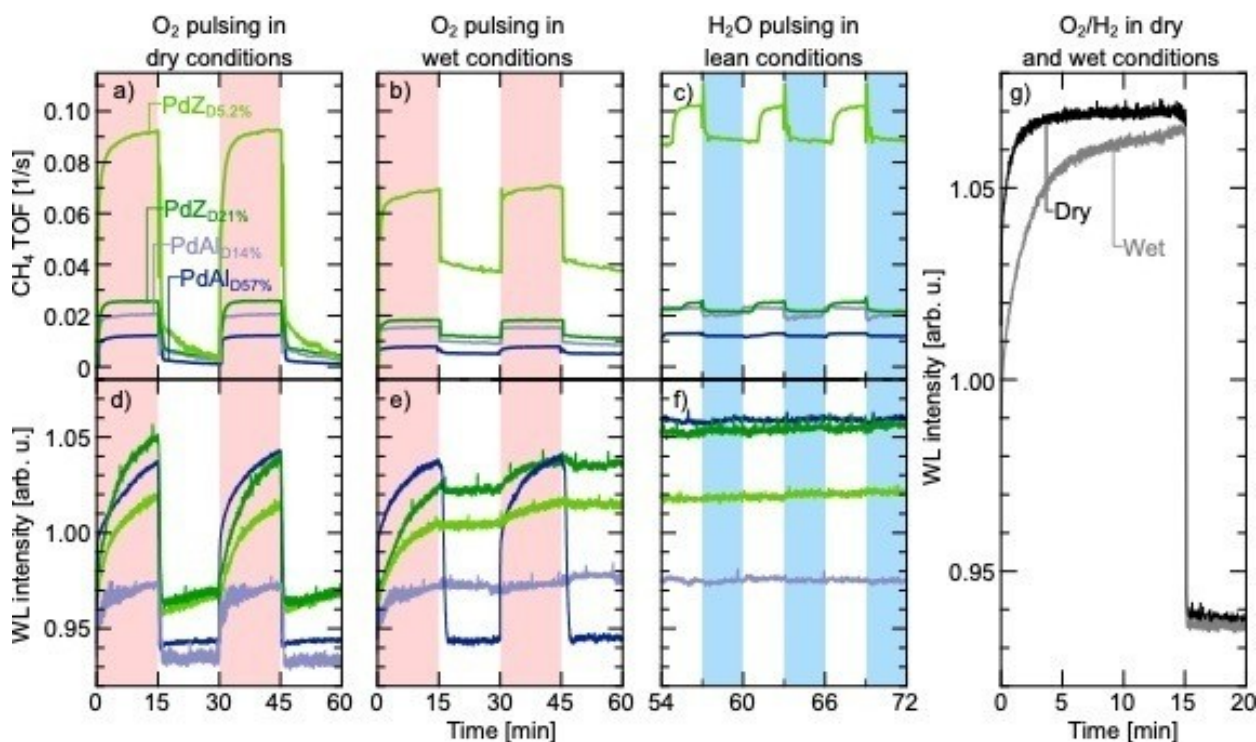


**Figure 3.** Operando ED-XAS measurements of Pd K edge WLI for the PdZr<sub>0.2</sub>1%, PdZr<sub>0.5</sub>2%, PdAl<sub>0.57</sub>% and PdAl<sub>0.14</sub>% samples at 360 °C during O<sub>2</sub> pulses to a CH<sub>4</sub>/He mixture (a and d), O<sub>2</sub> pulses to a CH<sub>4</sub>/H<sub>2</sub>O/He mixture (b and e), H<sub>2</sub>O pulses to a CH<sub>4</sub>/O<sub>2</sub>/He mixture (c and f) and for the PdAl<sub>0.57</sub>% during O<sub>2</sub>-H<sub>2</sub> cycling in dry and wet conditions (g).

360 °C. Upon introducing an O<sub>2</sub> pulse to the dry methane feed, the CH<sub>4</sub>-TOF increases for all catalysts due to the onset of total methane oxidation. Simultaneously, the WLI increases for all catalysts. The oxidation kinetics includes a rapid surface oxidation evidenced by the nearly stepwise increase in WLI at first, followed by a slower deep oxidation reflected by the asymptotic increase in WLI in line with previous results.<sup>[36]</sup> As a function of time on stream, the more dispersed catalysts reach higher WLIs. When O<sub>2</sub> is switched off, both CH<sub>4</sub>-TOF and WLI drop for all samples reflecting a rapid extinction of the methane oxidation reaction and fast reduction of the PdO particles. Moving to the case with O<sub>2</sub> pulses to the wet methane feed one first notices that although the CH<sub>4</sub>-TOFs and WLIs respond qualitatively similar to the corresponding dry cases, the TOFs are expectedly generally lower and the WLIs increase more slowly. The maximum WLIs are not reached until the second O<sub>2</sub> pulse has been effective. Thus, water slows down the oxidation of the palladium particles (this is clear also from the O<sub>2</sub>-H<sub>2</sub> cycling where the WLI increases more slowly in wet conditions (panel d)). When removing oxygen from the feed, the WLIs barely decrease, except for the well-dispersed alumina sample, which is in stark contrast to measurements in dry conditions. This suggests that only the smallest PdO particles are reduced by CH<sub>4</sub> in presence of water. During the oxygen-free periods, the measured CH<sub>4</sub>-TOF is due to the methane steam reforming producing hydrogen (H<sub>2</sub>) and carbon dioxide (CO<sub>2</sub>) as main products, which indicates that also the reverse water-gas shift reaction takes place. Finally, delving deeper into how water

impacts the PdO particles, the experiment with H<sub>2</sub>O pulses to a lean CH<sub>4</sub>/O<sub>2</sub> mixture clearly shows that the CH<sub>4</sub>-TOF decreases upon water addition for all catalysts but their corresponding WLI is (nearly) unchanged. Hence, water addition seems to preserve the palladium oxidation state while active sites become blocked for methane dissociation and lattice oxygens turn inactive for the methane oxidation (otherwise a decrease in WLI would be expected).

It is generally accepted that CH<sub>4</sub> oxidation on palladium oxide in oxygen excess conditions follows a Mars-van Krevelen mechanism and that water has a detrimental impact on the CH<sub>4</sub>-TOF as seen above.<sup>[13,33,46]</sup> Yet, no clear consensus on the mechanistic consequences of water has been reached, which may be due to the rich variation in catalyst systems and used analytical and theoretical tools. For supported palladium catalysts, Cullis *et al.* suggested that water transforms the active palladium oxide phase into an inactive palladium hydroxide phase.<sup>[47]</sup> Despite the low decomposition temperature of 250 °C for Pd(OH)<sub>2</sub>, which is lower than most temperatures used to study CH<sub>4</sub> oxidation, this explanation was used on speculative basis in many following studies.<sup>[9,48]</sup> Not until recently, Barret *et al.* showed its possible existence for supported catalysts at elevated temperatures using XAS measurements.<sup>[49]</sup> However, the formation of palladium hydroxide is likely limited to the surface region, in fact the amount of Pd(OH)<sub>2</sub> was shown to correlate with the Pd dispersion, and as such may be experimentally difficult to separate from hydroxyl, or other, ad-species.<sup>[49]</sup> Here, we consider the formation of a true Pd(OH)<sub>2</sub>

phase unlikely. Not only is the temperature higher than its decomposition temperature, no significant difference between the Pd K XAFS spectra for oxidized catalysts in dry and wet conditions could be seen. Instead, we attribute the water inhibition of lean methane oxidation to the formation of hydroxyl ad-species on the PdO particles. Calculations show that water can accumulate as hydroxyl ad-species on the active sites on the PdO(101) ideal surface at temperatures relevant for this study thereby blocking their catalytic function.<sup>[50]</sup> The corresponding experimental evidence has not yet been presented. However, in a recent study by Li *et al.* ambient-pressure X-ray photoelectron spectroscopy was used to show that water addition to a Pd foil at 350–600 °C leads to build-up of surface hydroxyls (and not palladium hydroxide) that block the methane dissociation and delay formation of active PdO.<sup>[51]</sup> Our results for realistic supported catalysts are in many respects analogous. Water addition impacts the dissociation of both CH<sub>4</sub> and O<sub>2</sub>, i.e., hampers the redox dynamics of the palladium particles, and seems to prevent lattice oxygens to take part in the methane oxidation reaction. Hence, we propose that the methane oxidation can no longer proceed by the Mars-van Krevelen mechanism but instead follow a Langmuir-Hinshelwood type of mechanism that becomes slower because of significant blockage of active sites and reaction with less active chemisorbed oxygen.<sup>[52]</sup> This knowledge is key in the search for new improved PdO-based catalyst concepts with clear implications on future technologies for low-temperature methane oxidation applications.

## Acknowledgements

The authors would like to thank the European Synchrotron Radiation Facility (ESRF) for providing the beamtime. This work was performed in part at the Chalmers Materials Analysis Laboratory, CMAL. The work was carried out within the Competence Centre for Catalysis, which is hosted by Chalmers University of Technology and financially supported by the Swedish Energy Agency and the member companies AB Volvo, ECAPS AB, Johnson Matthey AB, Preem AB, Scania CV AB, Umicore Denmark ApS, and Volvo Car Corporation AB. This work was funded by the Swedish Energy Agency through the FFI project "Fundamental studies on the influence of water on oxidation catalysts for biogas applications" (No. 40274-1).

## Conflict of Interest

The authors declare no conflict of interest.

**Keywords:** CH<sub>4</sub> activation · Catalyst design · Methane emission control · Operando characterization · Pd catalyst

[1] T. F. Stocker, D. Qin, G.-K. Plattner, M. Tignor, S. K. Allen, J. Boschung, A. Nauels, Y. Xia, V. Bex, P. M. Midgley, *Climate change 2013: The Physical*

*Science Basis. Contribution of Working Group I to the Fifth Assessment Report of the Intergovernmental Panel on Climate Change* **2013**, 1535.

- [2] J. J. West, A. M. Fiore, *Environ. Sci. Technol.* **2005**, *39*, 4685–4691.
- [3] A. Raj, *Johnson Matthey Technol. Rev.* **2016**, *60*, 228–235.
- [4] J. Merkisz, J. Pielecha, S. Radzimirski, *New Trends in Emission Control in the European Union*, Springer, **2014**.
- [5] T. Choudhary, S. Banerjee, V. Choudhary, *Appl. Catal. A* **2002**, *234*, 1–23.
- [6] P. Gélín, M. Primet, *Appl. Catal. B* **2002**, *39*, 1–37.
- [7] C. Coney, C. Stere, P. Millington, A. Raj, S. Wilkinson, M. Caracotsios, G. McCullough, C. Hardacre, K. Morgan, D. Thompson, *Catal. Sci. Technol.* **2020**, *10*, 1858–1874.
- [8] F. Ribeiro, M. Chow, R. Dallabetta, *J. Catal.* **1994**, *146*, 537–544.
- [9] R. Burch, F. Urbano, P. Loader, *Appl. Catal. A* **1995**, *123*, 173–184.
- [10] J. Van Giezen, F. Van den Berg, J. Kleinen, A. Van Dillen, J. Geus, *Catal. Today* **1999**, *47*, 287–293.
- [11] D. Ciuparu, N. Katsikis, L. Pfefferle, *Appl. Catal. A* **2001**, *216*, 209–215.
- [12] H. Nassiri, K.-E. Lee, Y. Hu, R. E. Hayes, R. W. Scott, N. Semagina, *J. Catal.* **2017**, *352*, 649–656.
- [13] P. Lott, P. Dolcet, M. Casapu, J.-D. Grunwaldt, O. Deutschmann, *Ind. Eng. Chem. Res.* **2019**, *58*, 12561–12570.
- [14] P. Velin, M. Ek, M. Skoglundh, A. Schaefer, A. Raj, D. Thompson, G. Smedler, P.-A. Carlsson, *J. Phys. Chem. C* **2019**, *123*, 25724–25737.
- [15] P. Velin, C.-R. Florén, M. Skoglundh, A. Raj, D. Thompson, G. Smedler, P.-A. Carlsson, *Catal. Sci. Technol.* **2020**, *10*, 5460–5469.
- [16] R. Gholami, M. Alyani, K. J. Smith, *Catalysts* **2015**, *5*, 561–594.
- [17] A. M. Beale, F. Gao, I. Lezcano-Gonzalez, C. H. F. Peden, J. Szanyi, *Chem. Soc. Rev.* **2015**, *44*, 7371–7405.
- [18] K. A. Karinshak, P. Lott, M. P. Harold, O. Deutschmann, *ChemCatChem* **2020**, *12*(14) 3712–3720.
- [19] N. M. Martin, J. Nilsson, M. Skoglundh, E. C. Adams, X. Wang, G. Smedler, A. Raj, D. Thompson, G. Agostini, S. Carlson, K. Norén, P.-A. Carlsson, *Catal. Struct. React.* **2017**, *3*(1–2), 24–32.
- [20] N. M. Martin, J. Nilsson, M. Skoglundh, E. C. Adams, X. Wang, P. Velin, G. Smedler, A. Raj, D. Thompson, H. H. Brongersma, T. Grehl, G. Agostini, O. Mathon, S. Carlson, K. Noreñ, F. J. Martinez-Casado, Z. Matej, O. Balmes, P.-A. Carlsson, *J. Phys. Chem. C* **2016**, *120*, 28009–28020.
- [21] S. Fouladvand, S. Schernich, J. Libuda, H. Grönbeck, T. Pingel, E. Olsson, M. Skoglundh, P.-A. Carlsson, *Top. Catal.* **2013**, *56*, 410–415.
- [22] P.-A. Carlsson, M. Skoglundh, *Appl. Catal. B* **2011**, *101*, 669–675.
- [23] P.-A. Carlsson, E. Fridell, M. Skoglundh, *Catal. Lett.* **2007**, *115*(1–2) 1–7.
- [24] S. Fouladvand, M. Skoglundh, P.-A. Carlsson, *Chem. Eng. Jour.* **2016**, *292*, 321–325.
- [25] R. J. Farrauto, M. Deeba, S. Alerasool, *Nature Catalysis* **2019**, *2*, 603–613.
- [26] P. A. Webb, C. Orr, *Analytical Methods in Fine Particle Technology*; Micromeritics Instrument Corporation, **1997**.
- [27] D. Tessier, A. Rakai, F. Bozon-Verduraz, *J. Chem. Soc. Farad. Trans.* **1992**, *88*, 741–749.
- [28] T. Lear, R. Marshall, J. A. Lopez-Sanchez, S. D. Jackson, T. M. Klapötke, M. Bäumer, G. Rupprechter, H.-J. Freund, D. Lennon, *J. Chem. Phys.* **2005**, *123*, 174706.
- [29] S. D. Ebbesen, B. L. Mojet, L. Lefferts, *Phys. Chem. Chem. Phys.* **2009**, *11*, 641–649.
- [30] N. M. Martin, M. Skoglundh, G. Smedler, A. Raj, D. Thompson, P. Velin, F. J. Martinez-Casado, Z. Matej, O. Balmes, P.-A. Carlsson, *J. Phys. Chem. C* **2017**, *121*, 26321–26329.
- [31] P. Gélín, A. R. Siedle, J. T. Yates Jr, *J. Phys. Chem.* **1984**, *88*, 2978–2985.
- [32] K. Okumura, E. Shinohara, M. Niwa, *Catal. Today* **2006**, *117*, 577–583.
- [33] W. R. Schwartz, L. D. Pfefferle, *J. Phys. Chem. C* **2012**, *116*, 8571–8578.
- [34] J. Nilsson, P.-A. Carlsson, S. Fouladvand, N. M. Martin, J. Gustafson, M. A. Newton, E. Lundgren, H. Grönbeck, M. Skoglundh, *ACS Catal.* **2015**, *5*, 2481–2489.
- [35] J. Nilsson, P.-A. Carlsson, N. M. Martin, A. C. Adams, G. Agostini, J. Grönbeck, M. Skoglundh, *J. Catal.* **2017**, *356*, 237–245.
- [36] J. Nilsson, P.-A. Carlsson, N. M. Martin, P. Velin, D. M. Meira, H. Grönbeck, M. Skoglundh, *Catal. Commun.* **2018**, *109*, 24–27.
- [37] M. Digne, P. Sautet, P. Raybaud, P. Euzen, H. Toulhoat, *J. Catal.* **2002**, *211*, 1–5.
- [38] M. Digne, P. Sautet, P. Raybaud, P. Euzen, H. Toulhoat, *J. Catal.* **2004**, *226*, 54–68.
- [39] G. Busca, *Catal. Today* **2014**, *226*, 2–13.
- [40] X. Liu, R. E. Truitt, *J. Am. Chem. Soc.* **1997**, *119*, 9856–9860.
- [41] H. Knözinger, P. Ratnasamy, *Catal. Rev. Sci. Eng.* **1978**, *17*, 31–70.
- [42] G. Busca, V. Lorenzelli, G. Ramis, R. J. Willey, *Langmuir* **1993**, *9*, 1492–1499.

- [43] K. Murata, J. Ohyama, Y. Yamamoto, S. Arai, A. Satsuma, *ACS Catal.* **2020**, *10*, 8149–8156.
- [44] G. Agostini, D. Meira, M. Monte, H. Vitoux, A. Iglesias-Juez, M. Fernández-García, O. Mathon, F. Meunier, G. Berruyer, F. Perrin, *J. Synchrotron Radiat.* **2018**, *25*, 1745–1752.
- [45] P. Velin, U. Stenman, M. Skoglundh, P.-A. Carlsson, *Rev. Sci. Instrum.* **2017**, *88*, 115102.
- [46] K.-I. Fujimoto, F. H. Ribeiro, M. Avalos-Borja, E. Iglesia, *J. Catal.* **1998**, *179*, 431–442.
- [47] C. Cullis, T. Nevell, D. Trimm, *J. Chem. Soc. Farad. Trans.* **1972**, *68*, 1406–1412.
- [48] D. Roth, P. Gélin, M. Primet, E. Tena, *Appl. Catal. A* **2000**, *203*, 37–45.
- [49] W. Barrett, J. Shen, Y. Hu, R. E. Hayes, R. W. Scott, *ChemCatChem* **2020**, *12*, 944–952.
- [50] M. van den Bossche, H. Grönbeck, *J. Am. Chem. Soc.* **2015**, *137*, 12035–12044.
- [51] X. Li, X. Wang, K. Roy, J. A. van Bokhoven, L. Artiglia, *ACS Catal.* **2020**, *10*, 5783–5792.
- [52] R. Burch, *Catal. Today* **1997**, *35*, 27–36.

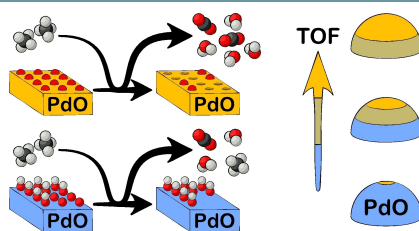
---

Manuscript received: June 8, 2021  
Revised manuscript received: June 29, 2021  
Accepted manuscript online: July 1, 2021  
Version of record online: ■■■, ■■■■

## COMMUNICATIONS

---

**Realistic Pd Catalyst:** Suppressed methane turn-over frequency caused by hydroxylation of active sites at the rim and on the supported PdO particles. The hydroxylation prevents lattice oxygen to take part in the reaction through inhibition and hampered PdO particle redox dynamics.



*Dr. P. Velin, F. Hemmingsson, Dr. A. Schaefer, Prof. M. Skoglundh, Dr. K. A. Lomachenko, Dr. A. Raj, Dr. D. Thompsett, Dr. G. Smedler, Prof. P.-A. Carlsson\**

1 – 8

**Hampered PdO Redox Dynamics by Water Suppresses Lean Methane Oxidation over Realistic Palladium Catalysts**

